

Article

Unbleached Nanofibrillated Cellulose as Additive and Coating for Kraft Paper

Elaine Cristina Lengowski ^{1,2,*} , Eraldo Antonio Bonfatti Júnior ³ , Leonardo Coelho Simon ²,
Vitória Maria Costa Izidio ¹, Alan Sulato de Andrade ^{4,5} , Silvana Nisgoski ⁴ and Graciela Inês Bolzon de Muniz ⁴

¹ Faculty of Forestry Engineering, Federal University of Mato Grosso, Fernando Corrêa da Costa Street, 2367, Cuiabá 78060-900, Brazil; vitoria.costaizidio@gmail.com

² Department of Chemical Engineering, University of Waterloo, 200 University Avenue West Waterloo, Waterloo, ON N2L 3G1, Canada; leonardo.simon@uwaterloo.ca

³ Department of Forest Engineering, Agrarian and Environmental Sciences Sector, Midwestern State University, Professor Maria Roza Zanon de Almeida Street, Irati 84505-677, Brazil; bonfattieraldo@gmail.com

⁴ Department of Engineering and Forestry Technology, Federal University of Paraná, Prefeito Lothário Meissner Avenue, 632, Curitiba 80210-170, Brazil; alansulato@gmail.com (A.S.d.A.); silvana.ufpr@gmail.com (S.N.); graciela.ufpr@gmail.com (G.I.B.d.M.)

⁵ School of Forest, Fisheries, and Geomatics Sciences, University of Florida, 136 Newins-Ziegler Hall, Gainesville, FL 32611-0410, USA

* Correspondence: elainelengowski@gmail.com or eclengow@uwaterloo.ca; Tel.: +55-41-99524-2675

Abstract: Although paper packages are biodegradable, their applications in food packaging are limited due to high affinity for absorbing moisture and the high permeability of gases and liquids with surroundings. Therefore, exploring the use biodegradable coatings such as nanocellulose to improve barrier is a relevant strategy. This study assessed the efficacy of unbleached nanofibrillated cellulose (NFC) as an additive to paper and coatings. Using NFC derived from unbleached eucalyptus pulp, a 5% mass addition to the paper pulp and a 2 mm wet nanocellulose coating to kraft paper handsheets made from pine pulp were investigated. In addition, nanocellulose films of similar thicknesses were appraised. The physical, morphological, mechanical, and thermal characteristics of the resulting papers were assessed. Incorporating NFC notably enhanced the morphology area of the paper by padding its pores, thus increasing its density by up to 48% and improving its water barrier properties by up to 50%. The mechanical strength showed significant enhancements, particularly in bursting and tensile strength with increases of up to 134% and 50%, respectively. Anyhow, the films exhibited lower bursting indices and no improvement in the tearing index. Nonetheless, the thermal stability of the handsheets with NFC coating meets the minimum requirements for food packaging.

Keywords: nanomaterials; food applications; barrier properties; mechanical properties; thermal stability



Citation: Lengowski, E.C.; Bonfatti Júnior, E.A.; Simon, L.C.; Izidio, V.M.C.; Andrade, A.S.d.; Nisgoski, S.; Muniz, G.I.B.d. Unbleached Nanofibrillated Cellulose as Additive and Coating for Kraft Paper. *Coatings* **2024**, *14*, 962. <https://doi.org/10.3390/coatings14080962>

Academic Editor: Isabel Coelho

Received: 27 May 2024

Revised: 1 July 2024

Accepted: 30 July 2024

Published: 1 August 2024



Copyright: © 2024 by the authors. Licensee MDPI, Basel, Switzerland. This article is an open access article distributed under the terms and conditions of the Creative Commons Attribution (CC BY) license (<https://creativecommons.org/licenses/by/4.0/>).

1. Introduction

Cellulosic materials with at least one dimension in the nanometer size can be classified as nanocellulose, regardless of their origin (vegetable or bacterial) or production method [1]. These nanomaterials can be classified into cellulose nanocrystals (CNC), cellulose microfibrils (CMF) and nanofibrillated cellulose (NFC) [2]. CNC are fully crystalline materials, whereas CMF and NFC contain regions of crystalline and amorphous cellulose, respectively [3–5]. CNC has applications in food packaging, water treatment, drug delivery, and in composites due to its rigidity [6]. CMF and NFC, which are flexible nanostructures, with greater length and contact area, are used in the development of food packaging, food additives, pigments, drug delivery, separation, nanocomposites, and several medical and pharmaceutical applications [6,7].

CMF and NFC are more suitable for producing paper because their amorphous regions can also create hydrogen bonds with paper fibers. CMF and NFC have diameters between 15 and 100 nm and 5 and 30 nm, with lengths varying between 0.5 and 20 µm, respectively [4,8].

Using NFC in the production of paper for food packaging is advantageous because of its natural origin, abundance, biodegradability, chemical compatibility with paper, and lightweight [4,9–15]. Moreover, it increases the mechanical properties of paper, improves its barrier properties, and does not change its density significantly [4,11,16]. Furthermore, NFC is biocompatible with food and does not leach harmful substances, and there is no evidence of carcinogenic, inflammatory, or cytotoxic effects of this nanomaterial [4,11,16].

Despite these advantages, using NFC in paper manufacturing presents operational and economic challenges. NFC production requires higher energy consumption and increases the drainage time and water removal during paper formation. Moreover, the retention of nanofibrils in the paper sheet can be difficult owing to the non-homogeneous dispersion and low fiber–nanofibril interaction. Furthermore, the interaction of NFC with other additives can cause undesirable effects on the paper characteristics, and conventional paper-forming machines are not suitable to use NFC as a drop-in additive [12,16–18].

Using nanocellulose as an additive is one of the numerous ways to combine nanocellulose with paper considering that it is possible to apply nanocellulose as a coating on already manufactured paper [10–13,15,19]. The application of nanocellulose coating to paper can be performed in several ways: (a) the best known method is spray coating, where a nanocellulose solution is sprayed directly on the surface of the paper; (b) bar coating is the process where nanocellulose is applied and spread on the surface of the paper using a coating bar; and (c) roll coating involves a roll which is dipped in the nanocellulose suspension and then rolled over the surface of the paper [17,20,21].

The application of nanocellulose to paper as a coating is the easiest and most explored method [1,15]. It requires a coating machine, which can be integrated with or without the paper machine; however, this also increases the cost of equipment installation. Therefore, evaluating the application of NFC as an additive in paper manufacturing is relevant because it could be the most economical method.

The present study aimed to compare the direct incorporation of unbleached NFC in paper manufacturing with the addition of an unbleached NFC coating on paper. The morphological characteristics, physical–mechanical properties, barrier properties, and thermal stability of the different papers manufactured were evaluated.

Bleached NFC has already been tested both as a coating and as an additive in paper-making [10,15], and showed unsatisfactory results in some properties, mainly in mechanical properties [15]. Bárta et al. [15] suggested the evaluation of unbleached NFC as a likely solution due to the greater presence of lignin; whereas Wang et al. [22] coated papers with layers of NFC and layers of lignin. In the present work, the new approach was to use unbleached NFC as both an additive and a coating.

2. Materials and Methods

2.1. Materials

In this study, paper handsheets were produced on a laboratory scale using unbleached pine kraft pulp with a kappa number of 62. The pulp was subjected to Schopper–Riegler refining to a level of 17°SR. Subsequently, paper handsheets were prepared using a Rapid-Köethen machine (Regmed, Osasco, Brazil) with a grammage of 60 g/m² [23]. Two distinct formation variations were considered: sheet production with only refined cellulosic pulp (TSN) and sheet production with the addition of 5% bleached nanofibrillated cellulose (NFC) to the refined pulp, amounting to the same final weight of 60 g/m² (TCN).

For the production of NFC, industrial unbleached eucalyptus kraft pulp, with a kappa number of 95.9, was used. A pulp solution with a consistency of 1% was prepared through homogenization in a blender. Subsequently, the pulp solution was processed in a Masuko Sangyo Super Masscollider MKCA6-2J (Masuko Sangyo, Kawaguchi, Japan) to convert it into a nanocellulose aqueous gel [24]. The solution was processed through the mill at a rotation speed of 1500 rpm for 10 passes.

2.2. Papers, Papers Coating, and Films Production

The paper-coating process relied on a casting solution method. NFC suspensions were applied to the paper sheets to form coatings with thicknesses of 1 and 2 mm. Following this, the paper sheets were first dried in an oven at 50 °C for 20 min and later in a Rapid-Köethen handsheet dryer at a temperature of 90 °C and pressure of 80 kPa [23]. Pure films were coated with 2-mm-thick layers of the NFC suspension, adopting the same coating application procedure.

In total, five distinct treatments were performed, each replicated 10 times. The resulting samples were labeled as follows:

- Kraft paper handsheet (sample KP);
- Uncoated kraft paper with nanocellulose on mass (sample KPN);
- Kraft paper with 2-mm of NFC surface application (sample KP2);
- Kraft paper with added NFC and a 2-mm-thick NFC surface coating (sample KPN2);
- NFC film with a thickness of 2 mm (sample F);

Before analysis, all samples were conditioned in a climate-controlled environment with a relative humidity of $50\% \pm 2\%$ and temperature of $23\text{ °C} \pm 2\text{ °C}$ [25].

2.3. Morphological Characterization

The morphological characterization of NFC was performed using transmission electron microscopy (TEM) with a JEOL JEM 1200EXII microscope at a magnification of $600\times$ (Jeol, Peabody, MA, USA). For this, the NFC suspension was diluted to 5 ppm using deionized water and subsequently deposited on 400-mesh grids. The samples were then allowed to air dry under ambient conditions. The diameters of the NFC fibers were recorded by taking three separate measurements from each TEM image.

Morphological examinations of the samples were performed using scanning electron microscopy with a HITACHI scanning microscope (model TM-1000) (HITACHI, Tokyo, Japan) and a Philips microscope (model XL 30 series) (Philips, Eindhoven, The Netherlands). To improve signal detection, the surfaces of the samples were metallized.

2.4. Physical and Barrier Characteristics

The physical properties of the samples were assessed by measuring their apparent density, water absorption capacity, and airflow resistance. The water absorption capacity was evaluated using the Cobb test [26], while airflow resistance was determined based on the Gurley air permeability test [27]. For NFC-coated papers, water absorption measurements were performed on both the coated and paper sides.

Furthermore, wettability was determined by measuring the contact angles of liquids on sample surfaces [28]. A Data Physics OCA goniometer, leveraging the sessile drop method, was adopted for these measurements at room temperature ($20\text{ °C} \pm 2\text{ °C}$). Three 5 μL droplets of deionized water and glycerol were deposited onto the samples, resulting in nine replicates for each solvent and sample type. Wettability kinetics were assessed by recording the contact angles immediately upon droplet contact with the sample (0) and after 5, 15, and 30 s of contact. These measurements were again conducted on both the coated and paper sides.

2.5. Mechanical Characteristics

The tensile strength of the samples was assessed according to the TAPPI T 494 om-13 standard [29]. A dynamometer was employed for the measurement, and the clamping distance was set to 50 mm. The tensile index was computed by correlating the tensile strength of the sample with its grammage. Next, burst resistance was measured following the TAPPI T 403 om-15 standard [30], with the burst index derived from the ratio of burst strength to grammage. Tear strength was quantified using the Elmendorf Pendulum equipment [31], while the tear index was calculated as the ratio of tear strength to grammage.

2.6. Thermal Characteristics

The thermal stability of NFC was assessed using thermogravimetric analysis (TGA) with a Setaram Setsys Evolution TGA/DSC (Setaram, Lyon, France) instrument. The TGA was conducted under an inert atmosphere with a flow rate of 40 mL/min, using a 5 mg sample. The treatment temperature ranged from 35 °C to 650 °C, with a heating rate of 10 °C/min. The resulting TG curve displayed mass loss as a function of temperature. Furthermore, the first derivative of this curve, known as the differential thermogravimetric curve, was used to determine the onset, maximum, and endpoint temperatures for thermal degradation. Mass losses within specific temperature ranges (100 °C–200 °C, 200 °C–300 °C, 300 °C–400 °C, 400 °C–500 °C, and 500 °C–600 °C) were computed utilizing the TG curves, offering insights into the initial, maximum, and final thermal degradation temperatures.

2.7. Statistical Analysis

The statistical analysis included several tests: the Grubbs test for identifying outliers, the Shapiro–Wilk test to assess data normality, Levene’s test to check for homogeneity of variance, and analysis of variance (ANOVA). When the equality hypothesis was rejected, Tukey’s mean comparison test was applied. The data were analyzed with the support of R software version 4.4.1 (The R Foundation for Statistical Computing, Vienna, Austria), with a probability level set at 95%.

3. Results

3.1. Morphological Analysis

Figure 1 shows the morphology of samples described in Section 2.2. The pine fibers initially exhibited micrometer-scale diameters (Figure 1A), ranging from 35 to 45 µm, with an average diameter of 40 µm. Through the refining process, these fibers underwent significant transformations, resulting in finer fibrillation of the cell wall (Figure 1B). Notably, the refining process facilitated the disintegration of cellulosic fibers into smaller units, increasing the available surface area for bonding—a crucial aspect of paper formation [32,33]. Following refining, both internal and external fibrillation were observed, causing the outer layers of the cell wall (the P and S1 layers) to delaminate and thus expose the S2 layer [34]. This led to the creation of nanoscale elements on the fiber surfaces, enhancing their properties. The addition of NFC further strengthened the interconnection between fibers owing to its numerous surface reactive hydroxyl sites (Figure 1C,D), which facilitated fiber approximation and bonding, similar to the refining process, as demonstrated by González et al. [35] and Zimmermann et al. [36] highlighted that the surface reactive sites of NFC engage in hydrogen bonding interactions with the fibers of the aqueous system used for paper production. Owing to the nanometric scale of NFC, the frequency and number of these hydrogen bonds are significantly increased by the greater contact surface area between the nanofibers and other fibers used in paper production.

The mechanical defibrillation process led to the defibrillation of the cell wall, converting the unbleached pulp into nanocelluloses. This process resulted in the delamination of the outer layers of the cell wall, beginning with the primary wall and extending to the secondary wall layers S1, S2, and S3 (Figure 2A) [34]. Micrograph analysis revealed that the unbleached NFC fibers exhibited an average diameter of 15.32 nm and varied in length over a few micrometers (Figure 2B).

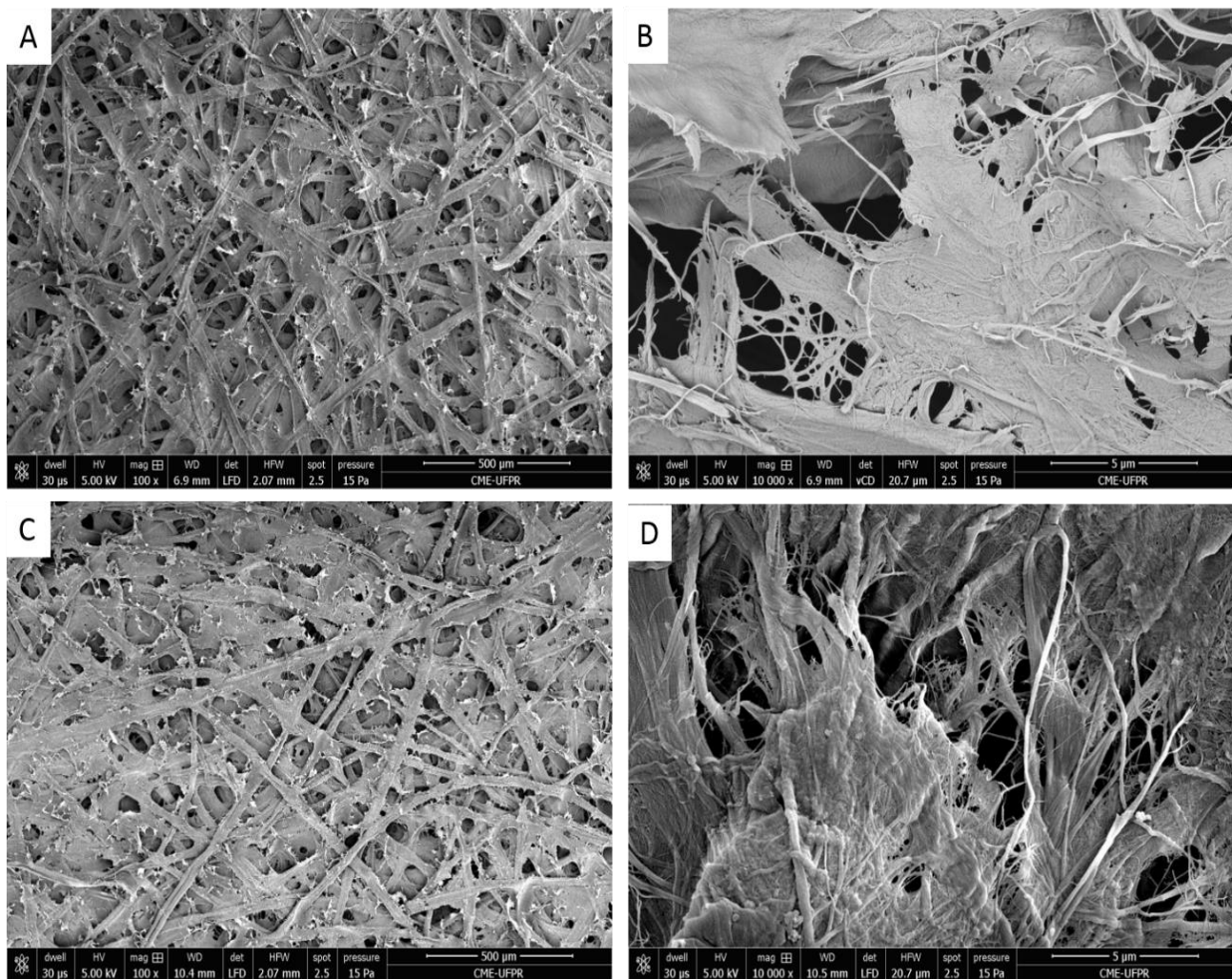


Figure 1. SEM images of kraft papers with nanocellulose on mass. (A) 100 \times magnification of the fibers that form the paper KP after refining; (B) 10,000 \times magnification of the nanometric fibrils formed by refining; (C) 100 \times magnification of the fibers that form the paper KPN after refining and add 5% off nanocellulose; (D) 10,000 \times magnification of the fibers that form the paper KPN after refining and add 5% off nanocellulose.

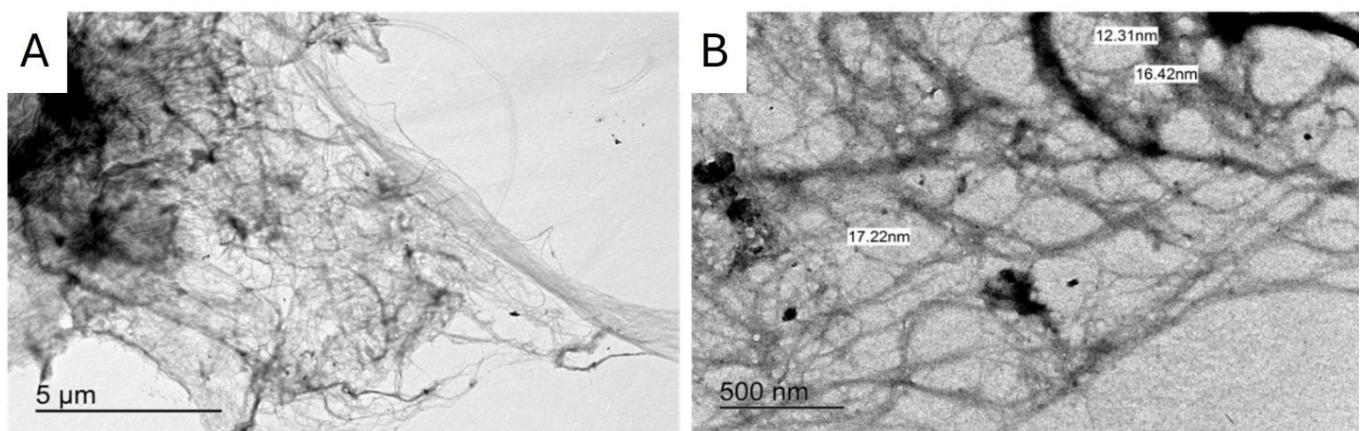


Figure 2. TEM. (A) Unbleached industrial eucalyptus kraft pulp NFC; (B) NFC produced with unbleached eucalyptus kraft pulp with measurements.

Treating the paper with NFC reduced its porosity, as the voids between the fibers were occupied by the added nanomaterial [37]. Notably, the increased surface area of NFC helps create a denser and more uniform paper surface. This improvement in the surface quality of paper is critical for its food packaging applications, as it directly impacts barrier properties and other essential characteristics [1,9,19]. As reduced porosity typically enhances barrier capabilities [22], the minimization of voids within paper marks a significant advancement in its application in food packaging. Pore filling was observed in both the KP2 and KPN2 samples (Figure 3). However, no significant differences in surface coatings between the two substrates (KP or KPN) were evident. Overall, the utilization of unbleached CMF created a more uniform film, attributed to lignin–cellulose interactions [10].

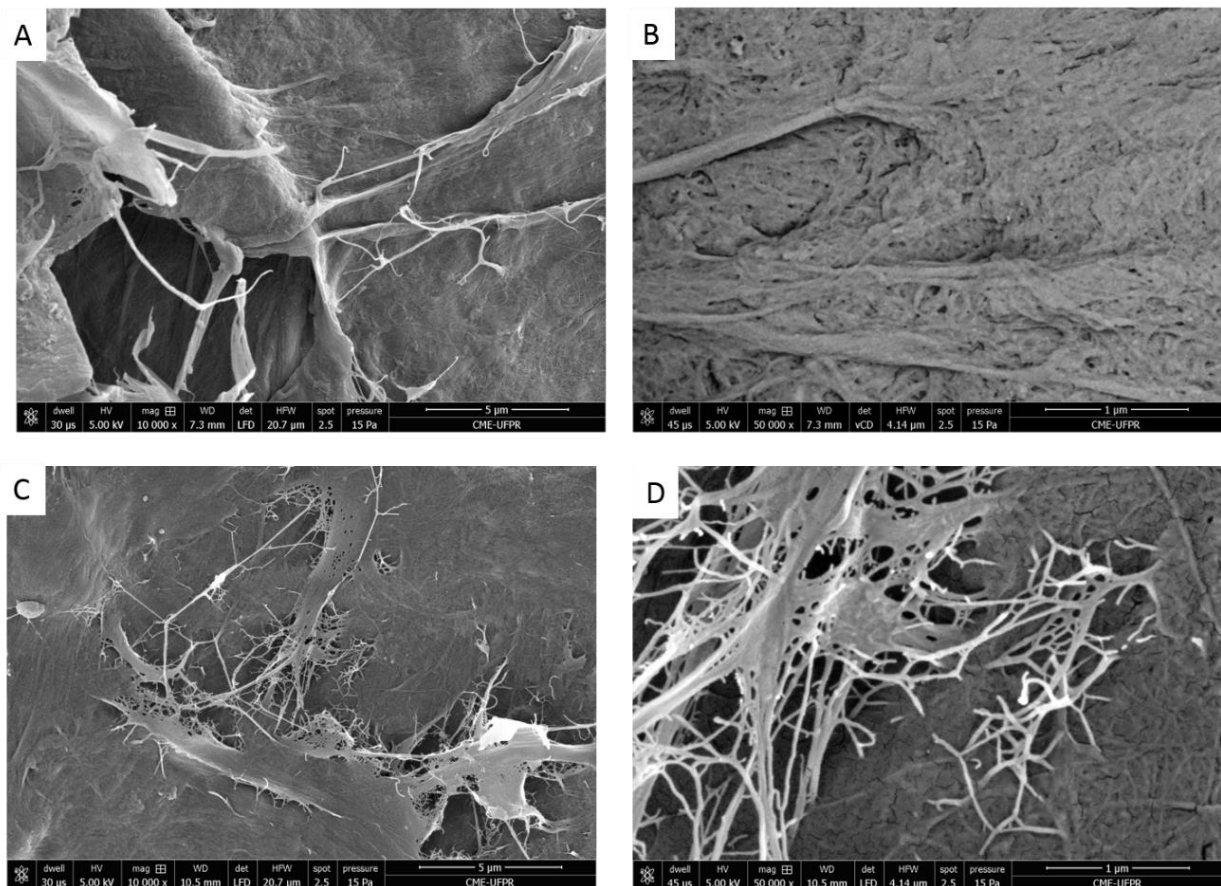


Figure 3. SEM images of kraft papers with nanocellulose coating. (A) 10,000× magnification of the paper KP2; (B) 50,000× magnification of the paper KP; (C) 10,000× magnification of the paper KPN (D) 50,000× magnification of the paper KPN2.

3.2. Physical and Barrier Characteristics

Applying coatings to paper led to a notable increase in its apparent density owing to the expanded contact surface of NFC and enhanced interactions and compaction between fibers [38] (Table 1). No significant differences in apparent density were observed between the KP2 and KPN2 samples. The surface density of a material is correlated with its porosity and barrier characteristics [21,38]. Owing to the nanometric size and enhanced interactions between the fibers of NFC, the NFC film demonstrated the highest apparent density; however, this density was still lower than that reported in the literature for bleached NFC films (approximately 1 g/cm²) [9,10].

Table 1. Apparent density and water absorption of papers, coated papers, and films.

Sample	Apparent Density (g/cm ³)	Water Absorption (g/m ²)
F	0.70 ± 0.05 c	45.84 ± 4.06 a
KPN	0.47 ± 0.29 a	130.72 ± 11.04 c
KP	0.44 ± 0.76 a	133.15 ± 5.19 c
KPN2 cs	0.64 ± 0.98 b	65.01 ± 2.98 b
KPN2 ps		203.28 ± 21.00 d
KP2 cs	0.65 ± 0.012 b	70.04 ± 11.83 b
KP2 ps		222.81 ± 22.08 d

cs: coating side. ps: paper side. Means followed by the different letters indicate statistical differences (Tukey test at 95% probability).

The coating applied to paper with nanocellulose (KPN2) increased its apparent density by 36% compared to the paper sample containing NFC only in its mass (KPN). Coating the paper sample devoid of NFC (KP2) increased its apparent density by 48% compared to the uncoated paper sample (KP). This effect was comparable to that of bleached NCF when added to kraft paper [10].

While the addition of NFC did not significantly reduce water absorption, the application of an NFC coating substantially reduced water absorption. For instance, the water absorption capacity of the KPN sample decreased by 50% after it was coated with the NCF film. Furthermore, the water absorption capacity of the KP sample decreased by 47.39% after it was coated with the NCF film (Table 1). Conversely, an unexpected increase in water absorption was observed on uncoated surfaces (labeled as ps on Table 1). For instance, the water absorption capacities of the KPN and KP samples were 130.72 g/m² and 133.15 g/m², respectively. However, following the application of the 2-mm-thick unbleached NFC film, the water absorption capacities of the paper sides of the KP2 and KPN2 samples increased to 222.81 g/m² and 203.28 g/m², respectively.

The high surface tension of NFC and the presence of abundant hydroxyl groups on its surface suggest that these fibers retain more water when exposed to surfaces compared to when applied as deposition coatings [38,39]. For instance, the average absorption capacity of the NFC film is 45.84 g/m², while that of the paper sample made solely from pulp (KP) is 133.15 g/m², 2.9 times higher than the former. This lower water absorption of the NFC film correlates with its reduced porosity and denser and more compact structure [38]. Additionally, owing to the hydrophobic nature of lignin, non-lignified NCF films tend to absorb more water, demonstrating a water absorption capacity between 60 and 115 g/m² [9].

The Cobb water absorption results over 60 s were comparable to those obtained for a paper sample coated with PLA over 30 s [40]. Notably, the sample coated with PLA absorbed 5 g of water in 30 s. Meanwhile, in this study, the coating sides of the KP2 and KPN2 samples absorbed 5.28 g and 4.90 g of water, respectively, in 60 s.

The air permeance values of the KP and KPN samples were measured to be 1.30 s/100 cm³ and 3.14 s/100 cm³, respectively. After applying NFC coatings, the top flow time of the air column (1800 s) was extrapolated for all samples, including the NFC film (sample F). This measurement indicated that the air flow resistances of the NFC film and coated paper samples were higher than the range determined through the Gurley air permeability test, indicating low permeability [9,41,42]. Thus, coating with NFC proved to be more efficient than coating with PLA, which demonstrated an air permeance of 93 s/100 cm³ [40].

During the water permeability assessments of all samples, including the uncoated paper, coated paper, and film samples, contact angles decreased (Table 2). For instance, the contact angle of water on the NFC film (sample F) decreased. A similar trend was observed for the coated sides of samples KPN2 and KP2. Conversely, for samples KPN and KP, water droplets were absorbed almost immediately, and contact angle measurements were not possible after 15 s. Furthermore, water absorption occurred almost instantly on the side opposite to the NFC coating.

Table 2. Kinetics of contact angle using water.

Sample	0 s	5 s	15 s	30 s
F	73.15 ± 5.79 ab	64.09 ± 9.33 b	60.32 ± 12.89 a	57.04 ± 15.55 a
KPN	70.36 ± 22.98 ab	73.5 ± 15.11 b	0	0
KP	65.36 ± 7.77 a	18.45 ± 5.58 a	0	0
KPN2 cs	73.04 ± 13.00 ab	59.77 ± 14.96 b	56.68 ± 15.74 a	55.01 ± 16.00 a
KPN2 ps	81.64 ± 7.38 bc	36.8 ± 10.42 a	0	0
KP2 cs	74.42 ± 6.72 ab	63.00 ± 9.79 b	62.2 ± 11.02 a	60.57 ± 12.64 a
KP2 ps	90.07 ± 7.99 c	50.28 ± 17.53 ab	0	0

cs: coating side, ps: paper side. Means followed by the different letters indicate statistical differences (Tukey test at 95% probability).

Generally, to facilitate processing, nanocelluloses are produced from bleached pulp, which exhibits hydrophilic properties and yields films with poor water barrier characteristics. This poses challenges for the incorporation of nanocelluloses within food packaging materials. However, lignin-containing nanocelluloses may offer advantages, such as reduced operating costs and better resistance and barrier characteristics attributed to the hydrophobic nature of lignin [43]. Spence et al. [38] reported an initial contact angle of 50.8°, which increased with increasing lignin content in films made from unbleached short-fiber pulp. The authors concluded that lignin, being more hydrophobic than cellulose, resulted in a higher initial contact angle.

The wettability of the samples was assessed by measuring the contact angle between a liquid droplet and the sample substrates. The contact angle is defined as the angle formed by the tangent with the gas–liquid interface where the droplet encounters the solid surface and the contact angle of the gas–solid–liquid system stabilizes. Typically, a smaller angle indicates better wettability of the substrate [44].

The contact angle was observed to decrease over time, partially attributed to the viscosity and molecular characteristics of glycerol (Table 3). For sample F, the coated side of sample KPN2, and the coated side of sample KP, surface spreading of droplets was noted. Conversely, for sample KP, the paper side of sample KPN2, and the paper side of sample KP2, the droplets were absorbed, resulting in paper swelling. Following coating application, minimal variations in wettability were observed, suggesting that the application of NFC coatings made the surface less prone to wetting. Furthermore, the addition of NFC to the pulp during paper production did not significantly alter wettability, whether evaluated on the paper side or the coated side.

Table 3. Kinetics of contact angle using glycerol.

Sample	0 s	5 s	15 s	30 s
F	89.45 ± 8.52 a	53.68 ± 10.73 ab	41.88 ± 9.73 ab	33.43 ± 8.32 ab
KPN	90.43 ± 9.13 a	54.57 ± 14.56 abc	36.53 ± 11.80 a	27.4 ± 9.46 a
KP	86.56 ± 8.26 a	49.01 ± 6.60 a	35.88 ± 6.70 a	37.02 ± 10.97 a
KPN2 cs	95.45 ± 4.98 ab	71.36 ± 8.66 d	57.79 ± 7.92 c	43.74 ± 12.33 bc
KPN2 ps	94.14 ± 8.54 ab	65.74 ± 11.65 bcd	50.52 ± 13.45 bc	47.84 ± 6.43 c
KP2 cs	89.75 ± 9.48 a	52.02 ± 9.98 ab	39.8 ± 9.17 ab	42.68 ± 5.76 bc
KP2 ps	102.35 ± 5.97 b	67.36 ± 7.88 cd	50.68 ± 11.06 bc	32.8 ± 8.00 ab

cs: coating side, ps: paper side. Means followed by the different letters indicate statistical differences (Tukey test at 95% probability).

The contact angle values for water are similar to those reported for biopolymers such as poly(butylene succinate) (78.6°–89.9°) [45,46] and poly(lactic acid) (69° and 44°) [46]. Generally, smoother surfaces exhibit lower contact angles compared to rougher ones [43]. The structures of nanocellulose films and coatings are significantly more compact, better inhibiting the penetration of water and glycerol compared to pure kraft paper samples [47].

Surface energy refers to the increase in free energy per unit area when a new surface is created. The Owens–Wendt–Kaelble method states that the surface energy of hydrophobic

substrates can be regulated through two primary strategies: The first strategy involves modifying rough substrates with materials featuring low surface energies, while the second strategy involves creating hierarchical structures at both micro- and nano-scales on hydrophobic surfaces [47,48]. In this study, when NCF was added to the mass or applied as a coating, the roughness and porosity of the resulting samples decreased. This increased their surface energy and enhanced their hydrophobicity.

The Fowkes method [49] posits that the surface tension of a liquid and the free energy of a solid surface comprise two primary components: intermolecular dispersion forces (primarily involving interactions among non-polar molecules) and polarity components (primarily including dipole interactions and hydrogen bonds, whose strength is influenced by the polarity factor of the surface). Both water and glycerol are polar substances; however, water is more polar owing to its simple structure and higher dipole moment, resulting from the greater electronegativity difference between the hydrogen and oxygen atoms. Polar liquids tend to interact more strongly with polar surfaces. Consequently, water, being polar, forms hydrogen bonds with polar groups on solid surfaces and is absorbed quickly. Conversely, glycerol is less absorbent than water owing to its low polarity. Furthermore, glycerol has a higher surface tension (64 mN/m) compared to water (72 mN/m, at 20 °C), which makes it more difficult for glycerol to be absorbed by the paper surface [50].

Thermoformed pulp food packaging is gaining traction worldwide as an alternative to expanded polystyrene and other plastic packaging materials [51,52]. Typically, mechanical pulps with low barrier and mechanical resistance are used for this purpose [51]. For pulp-molded tableware, functional chemicals such as oil-resistant, water-resistant, and retention agents are added to the mechanical pulps [52]. Furthermore, nanocellulose additives have been tested to improve the properties of mechanical pulps [51]. In the United States and Europe, stringent standards govern the choices of food packaging paper, with chlorine-bleached pulp being strictly prohibited owing to safety concerns [51,52]. Instead, industrial applications often prefer safer alternatives such as chlorine-free bleaching treatments. Unbleached nanocellulose is used in these applications to enhance both barrier and mechanical properties [32,53].

3.3. Mechanical Characteristics

Mechanical characteristics were affected by the nanocellulose coatings (Table 4).

Table 4. Mechanical characteristics of papers, coated papers, and film.

Sample	Burst Index (kPa·m ² /g)	Tear Index (mN·m ² /g)	Tensile Index (N·m/g)
F	3.14 ± 0.44 c		89.90 ± 18.35 a
KPN	6.76 ± 0.35 b	22.49 ± 0.00 b	86.83 ± 12.12 a
KP	4.34 ± 0.17 c	17.67 ± 0.71 c	60.56 ± 3.33 b
KPN2	10.17 ± 0.65 a	25.41 ± 1.08 a	90.95 ± 5.05 a
KP2	6.61 ± 1.63 b	21.67 ± 1.05 b	70.03 ± 5.47 b

Means followed by the different letters indicate statistical differences (Tukey test at 95% probability).

Samples F and KP exhibited lower burst indices compared to the KPN, KP2, and KPN2 samples, presenting differences of 56%, 52%, and 134%, respectively. Notably, the burst index of the KPN sample, which contained NFC in its mass, was similar to that of the KP2 sample, which was devoid of NFC in its mass but was coated with NFC. However, sample F displayed a lower burst index compared to the KP, KPN, KP2, and KPN2 samples.

The tear index increased with the addition of NFC. For instance, compared to the tear index of the KP sample, those for KPN, KP2, and KPN2 increased by 27%, 23%, and 50%, respectively. Similar to the previous case, the tear index of the KPN sample, which contained NFC in its mass, was similar to that of the KP2 sample, which was devoid of NFC in its mass but was coated with NFC. Conversely, sample F exhibited no tearing property, as its thickness was greatly reduced during the fibrillation process [9].

The tensile index improved with the application of NFC. For instance, compared to the tensile index of the KP sample, those of the KPN, KP2, and KPN2 samples increased by 43%, 16%, and 50%, respectively. Furthermore, the tensile resistance of sample F was similar to the resistances of the KPN and KPN2 samples. This behavior was also apparent for the KP and KP2 samples, where the coating did not enhance this property.

The mechanical refining of unbleached cellulosic pulp from *Pinus* sp. can double the burst index [54]; however, in this study, only the coating treatment applied to the sample containing NCF in its mass (KPN2) overcame the refining effect. For the tensile index, mechanical refining is less effective, with improvements not exceeding 10% [54]. Thus, the addition of NFC offers more substantial improvements in the tensile resistance compared to the refining of cellulosic pulp. The anticipated enhancement in tensile and bursting strength with nanocellulose is associated with the degree of fiber interlacing and fiber length [9]. However, the contribution of fiber interlacing is less pronounced, as this property heavily relies on the cell wall thickness [9,21,55].

When comparing kraft paper samples coated with similar thicknesses of bleached nanocellulose, Lengowski et al. [10] reported greater gains in the tensile and burst indices and lower tear index values than those observed in this study. The mechanical properties analyzed here exhibited a different trend. For thermoformed packaging, the addition of lignin during thermoforming reduces voids within the fiber network, weakens the load stress transfer capacity, and improves fiber plasticity [56].

3.4. Thermal Stability

Table 5 reports the data for thermal stability. Thermal mass loss in the samples initiated at temperatures above 200 °C. Samples KP and KPN exhibited greater thermal stability compared to the samples with surface coatings up to 300 °C (Figure 4 and Table 5). Beyond this temperature, the coated samples (KP2 and KPN2) and film (F) exhibited low mass losses.

Table 5. Thermal degradation of papers, coated papers, and film.

Sample	Mass Loss (%)				
	100–200 °C	200–300 °C	300–400 °C	400–500 °C	After 500 °C
F	0.19	9.11	53.60	3.85	33.25
KP	0.38	4.15	65.11	3.26	29.10
KPN	0.13	3.26	64.06	3.36	29.19
KP2	1.18	6.29	57.62	4.47	30.45
KPN2	0.72	6.93	56.99	4.35	31.01

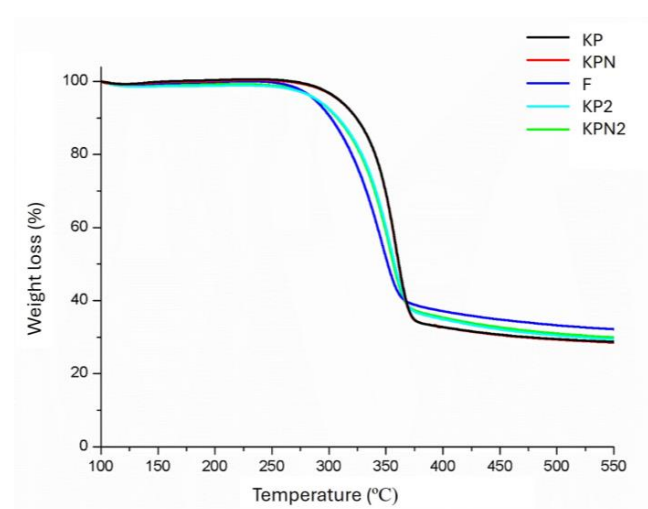


Figure 4. Temperature evolution and weight loss of papers, coated papers, and film.

Sample F demonstrated the lowest thermal stability below 300 °C. In the 300 °C–400 °C range, the uncoated samples exhibited the lowest thermal stability. NFC addition to the mass slightly reduced the thermal stability below 300 °C.

These changes in thermal stability can be attributed to the increased bonding between the fibrils, which enhances the thermal stability of the films [9]. Similar results have been reported for kraft papers coated with bleached NFC; however, at temperatures exceeding 300 °C, the presence of lignin improved the thermal stability of both films and coatings [10].

In this study, the thermal stability of the samples was influenced by both the addition of NFC to the sample mass and application of NFC coatings. The presence of nanocellulose increased the onset temperature for thermal degradation, owing to the formation of a denser network and stronger bonding between the fibers, which enhanced thermal stability (Table 6).

Table 6. Temperature intervals at which thermal degradation occurs.

Sample	Thermal Degradation Temperatures (°C)		
	T _{onset}	T _{max}	T _{endset}
F	227	347	411
KP	226	359	390
KPN	238	359	387
KP2	235	355	392
KPN2	244	354	390

T_{onset}: onset of thermal decomposition temperature. T_{max}: maximum mass variation temperature. T_{endset}: end of thermal decomposition temperature.

Materials intended for food packaging must withstand temperatures ranging from −40 °C to 220 °C [57]. Although the onset temperature for thermal degradation (T_{onset}) in the tested materials is lower than that of common packaging plastics, such as polypropylene, polystyrene, polyethylene terephthalate, poly(lactic acid), and poly(butylene succinate) [58–61], NFC addition does not compromise the thermal stability of the samples. Compared to bleached NCF films, the T_{onset} and T_{max} values of the unbleached NCF films and coatings are similar; however, the T_{endpoint} of bleached NCF is considerably lower (T_{endpoint}: 283 °C) [10].

4. Conclusions

The utilization of NFC as an additive incorporated in the sample mass and as a coating applied to the surfaces of paper samples significantly enhanced the performance of kraft paper. This improvement is particularly advantageous for food packaging, as NCF addition reduced the porosity of kraft paper handsheets and increased their apparent density by approximately 48%. Notably, water and glycerol absorption decreased on the coated sides of the samples but increased on the paper sides. NFC addition to the sample mass reduced the water absorption capacity of the samples by 1.82%, whereas applying it as a coating reduced the water absorption capacity by approximately 50%.

For applications requiring enhanced mechanical properties, incorporating NFC into the pulp provides a straightforward production solution. Coating with NFC notably enhanced tearing (up to 50%) and bursting properties (up to 134%). Although incorporating NFC into the pulp decreased air permeability, it did not achieve the waterproofing effect observed with coating deposition.

All tested materials demonstrated adequate thermal stability for food packaging, with the onset temperature of thermal degradation exceeding 220 °C.

Future research must seek strategies to facilitate the production of papers with enhanced barrier properties through the addition of NFC to cellulosic pulp. Future studies on food migration and cytotoxicity are essential to validate the applicability of NFC in primary packaging production. Furthermore, testing integrated applications, such as the use of low mechanical pulp in thermoformed pulp, could offer additional insights.

Nanocellulose demonstrates promise as a biodegradable material for use in bioplastics, potentially replacing non-biodegradable polymers. Its application either as an additive, a layer, or a coating can improve gas and liquid barrier properties, as well as mechanical properties. This study concludes that applying NFC as a layer or coating can significantly enhance the barrier properties of kraft paper samples, but further research is needed to explore its full potential.

Author Contributions: Conceptualization, E.C.L., L.C.S. and G.I.B.d.M.; methodology, E.C.L.; formal analysis, A.S.d.A., V.M.C.I. and S.N.; investigation, E.C.L., V.M.C.I. and E.A.B.J.; resources, E.C.L. and E.A.B.J.; data curation, E.C.L. and E.A.B.J.; writing—original draft preparation, E.C.L. and E.A.B.J.; writing—review and editing, E.C.L. and E.A.B.J.; visualization, A.S.d.A.; supervision, E.C.L., L.C.S., A.S.d.A., S.N. and G.I.B.d.M.; project administration, E.C.L.; funding acquisition, E.C.L., E.A.B.J., G.I.B.d.M. and L.C.S. All authors have read and agreed to the published version of the manuscript.

Funding: This study was financed in part by Brazil's Office to Improve University Personnel (CAPES), Finance Code 001, and by the National Council for Scientific and Technological Development (CNPq); FAPEMAT.0000077/2022.

Institutional Review Board Statement: Not applicable.

Informed Consent Statement: Not applicable.

Data Availability Statement: Data are contained within the article.

Acknowledgments: The authors are grateful to the Pulp and Paper Laboratory team from Federal University of Paraná for all their support with this paper and to the Electron Microscopy Center (CME-UFPR), FANUT, UFMT, University of Waterloo, Klabin and FAPEMAT.

Conflicts of Interest: The authors declare no conflicts of interest.

References

1. Lengowski, E.C.; Bonfatti Júnior, E.A.; Kumode, M.M.N.; Carneiro, M.E.; Satyanarayana, K.G. Nanocellulose in the Paper Making. In *Sustainable Polymer Composites and Nanocomposites*; Inamuddin, Thomas, S., Kumar Mishra, R., Asiri, A.M., Eds.; Springer International Publishing: Cham, Switzerland, 2019; pp. 1027–1066. ISBN 978-3-030-05398-7.
2. Fernandes, A.; Cruz-Lopes, L.; Esteves, B.; Evtuguin, D. Nanotechnology Applied to Cellulosic Materials. *Materials* **2023**, *16*, 3104. [\[CrossRef\]](#)
3. Kassab, Z.; Abdellaoui, Y.; Salim, M.H.; Bouhfid, R.; Qaiss, A.E.K.; El Achaby, M. Micro- and Nano-Celluloses Derived from Hemp Stalks and Their Effect as Polymer Reinforcing Materials. *Carbohydr. Polym.* **2020**, *245*, 116506. [\[CrossRef\]](#) [\[PubMed\]](#)
4. Lengowski, E.C.; Franco, T.S.; Viana, L.C.; Bonfatti Júnior, E.A.; De Muñoz, G.I.B. Micro and Nanoengineered Structures and Compounds: Nanocellulose. *Cellulose* **2023**, *30*, 10595–10632. [\[CrossRef\]](#)
5. Noremylia, M.B.; Hassan, M.Z.; Ismail, Z. Recent Advancement in Isolation, Processing, Characterization and Applications of Emerging Nanocellulose: A Review. *Int. J. Biol. Macromol.* **2022**, *206*, 954–976. [\[CrossRef\]](#)
6. Poulouse, A.; Parameswaranpillai, J.; George, J.J.; Gopi, J.A.; Krishnasamy, S.; Dominic, C.D.M.; Hameed, N.; Salim, N.V.; Radoor, S.; Sienkiewicz, N. Nanocellulose: A Fundamental Material for Science and Technology Applications. *Molecules* **2022**, *27*, 8032. [\[CrossRef\]](#) [\[PubMed\]](#)
7. Barhoum, A. *Handbook of Nanocelluloses: Classification, Properties, Fabrication, and Emerging Applications*; Springer: Cham, Switzerland, 2022. [\[CrossRef\]](#)
8. Sehaqui, H.; Allais, M.; Zhou, Q.; Berglund, L.A. Wood Cellulose Biocomposites with Fibrous Structures at Micro- and Nanoscale. *Compos. Sci. Technol.* **2011**, *71*, 382–387. [\[CrossRef\]](#)
9. Lengowski, E.C.; Bonfatti Júnior, E.A.; Simon, L.; De Muñoz, G.I.B.; De Andrade, A.S.; Nisgoski, S.; Klock, U. Different Degree of Fibrillation: Strategy to Reduce Permeability in Nanocellulose-Starch Films. *Cellulose* **2020**, *27*, 10855–10872. [\[CrossRef\]](#)
10. Lengowski, E.C.; Bonfatti Júnior, E.A.; Coelho Simon, L.; Bolzon De Muniz, G.I.; Sulato De Andrade, A.; Neves Leite, A.; Souza De Miranda Leite, E.L. Nanocellulose Coating on Kraft Paper. *Coatings* **2023**, *13*, 1705. [\[CrossRef\]](#)
11. Xu, Y.; Wu, Z.; Li, A.; Chen, N.; Rao, J.; Zeng, Q. Nanocellulose Composite Films in Food Packaging Materials: A Review. *Polymers* **2024**, *16*, 423. [\[CrossRef\]](#)
12. Hashemzahi, M.; Mesic, B.; Sjöstrand, B.; Naqvi, M. A Comprehensive Review of Nanocellulose Modification and Applications in Papermaking and Packaging: Challenges, Technical Solutions, and Perspectives. *BioResources* **2022**, *17*, 3718–3780. [\[CrossRef\]](#)
13. Li, A.; Xu, D.; Luo, L.; Zhou, Y.; Yan, W.; Leng, X.; Dai, D.; Zhou, Y.; Ahmad, H.; Rao, J.; et al. Overview of Nanocellulose as Additives in Paper Processing and Paper Products. *Nanotechnol. Rev.* **2021**, *10*, 264–281. [\[CrossRef\]](#)

14. Zambrano, F.; Starkey, H.; Wang, Y.; Abbati De Assis, C.; Venditti, R.; Pal, L.; Jameel, H.; Hubbe, M.A.; Rojas, O.J.; Gonzalez, R. Using Micro- and Nanofibrillated Cellulose as a Means to Reduce Weight of Paper Products: A Review. *BioResources* **2020**, *15*, 4553–4590. [[CrossRef](#)]
15. Bárta, J.; Hájková, K.; Sikora, A.; Jurczykova, T.; Popelková, D.; Kalous, P. Effect of a Nanocellulose Addition on the Mechanical Properties of Paper. *Polymers* **2023**, *16*, 73. [[CrossRef](#)] [[PubMed](#)]
16. Cañas-Gutiérrez, A.; Gómez Hoyos, C.; Velásquez-Cock, J.; Gañán, P.; Triana, O.; Cogollo-Flórez, J.; Romero-Sáez, M.; Correa-Hincapié, N.; Zuluaga, R. Health and Toxicological Effects of Nanocellulose When Used as a Food Ingredient: A Review. *Carbohydr. Polym.* **2024**, *323*, 121382. [[CrossRef](#)] [[PubMed](#)]
17. Das, A.K.; Islam, M.N.; Ashaduzzaman, M.; Nazhad, M.M. Nanocellulose: Its Applications, Consequences and Challenges in Papermaking. *J. Packag. Technol. Res.* **2020**, *4*, 253–260. [[CrossRef](#)]
18. Salas, C.; Hubbe, M.; Rojas, O.J. Nanocellulose Applications in Papermaking. In *Production of Materials from Sustainable Biomass Resources*; Fang, Z., Smith, R.L., Jr., Tian, X.-F., Eds.; Biofuels and Biorefineries; Springer: Singapore, 2019; Volume 9, pp. 61–96. ISBN 9789811337673.
19. Spagnuolo, L.; D’Orsi, R.; Operamolla, A. Nanocellulose for Paper and Textile Coating: The Importance of Surface Chemistry. *ChemPlusChem* **2022**, *87*, e202200204. [[CrossRef](#)] [[PubMed](#)]
20. Liu, W.; Liu, K.; Du, H.; Zheng, T.; Zhang, N.; Xu, T.; Pang, B.; Zhang, X.; Si, C.; Zhang, K. Cellulose Nanopaper: Fabrication, Functionalization, and Applications. *Nano-Micro Lett.* **2022**, *14*, 104. [[CrossRef](#)] [[PubMed](#)]
21. Tarrés, Q.; Aguado, R.; Pèlach, M.À.; Mutjé, P.; Delgado-Aguilar, M. Electro spray Deposition of Cellulose Nanofibers on Paper: Overcoming the Limitations of Conventional Coating. *Nanomaterials* **2021**, *12*, 79. [[CrossRef](#)]
22. ISO 5269-2:2004; Pulps—Preparation of Laboratory Sheets for Physical Testing—Part 2: Rapid-Köthen Method. International Standardization Organization: Geneva, Switzerland, 2008.
23. Magalhães, W.L.E.; Claro, F.C.; Matos, M.; Lengowski, E.C. *Produção de Nanofibrilas de Celulose por Desfibrilação Mecânica em Moinho Coloidal*; Embrapa Florestas: Colombo, Brazil, 2017.
24. TAPPI T 402 sp-13; Standard Conditioning and Testing Atmospheres for Paper, Board, Pulp Handsheets, and Related Products. Technical Association of Pulp and Paper Industry: Atlanta, GA, USA, 2013.
25. TAPPI T 220 sp-16; Physical Testing of Pulp Handsheets. Technical Association of Pulp and Paper Industry: Atlanta, GA, USA, 2016.
26. TAPPI T 441 om-20; Water Absorptiveness of Sized (Non-Bibulous) Paper, Paperboard, and Corrugated Fiberboard (Cobb Test). Technical Association of Pulp and Paper Industry: Atlanta, GA, USA, 2020.
27. TAPPI T 460 om-16; Air Resistance of Paper (Gurley Method). Technical Association of Pulp and Paper Industry: Atlanta, GA, USA, 2016.
28. ASTM D7334-08; Standard Practice for Surface Wettability of Coatings, Substrates and Pigments by Advancing Contact Angle Measurement. American Society for Testing and Materials: West Conshohocken, PA, USA, 2022.
29. TAPPI T 494 om-22; Tensile Properties of Paper and Paperboard (Using Constant Rate of Elongation Apparatus). Technical Association of Pulp and Paper Industry: Atlanta, GA, USA, 2022.
30. TAPPI T 403 om-22; Bursting Strength of Paper. Technical Association of Pulp and Paper Industry: Atlanta, GA, USA, 2023.
31. TAPPI T 414 om-21; Internal Tearing Resistance of Paper (Elmendorf-Type Method). Technical Association of Pulp and Paper Industry: Atlanta, GA, USA, 2021.
32. Swinehart, D. *Fundamentals of Refining*; MeadWestvaco Center for Packaging Innovation: Richmond, VA, USA, 2012.
33. Nakagaito, A.N.; Yano, H. The effect of morphological changes from pulp fiber towards nano-scale fibrillated cellulose on the mechanical properties of high-strength plant fiber based composites. *Appl. Phys. A* **2004**, *78*, 547–552. [[CrossRef](#)]
34. González, I.; Boufi, S.; Pèlach, M.A.; Alcalà, M.; Vilaseca, F.; Mutjé, P. Nanofibrillated cellulose as paper additive in Eucalyptus pulps. *BioResources* **2012**, *7*, 5167–5180. [[CrossRef](#)]
35. Zimmermann, T.; Bordeanu, N.; Strub, E. Properties of Nanofibrillated Cellulose from Different Raw Materials and Its Reinforcement Potential. *Carbohydr. Polym.* **2010**, *79*, 1086–1093. [[CrossRef](#)]
36. Balea, A.; Monte, M.C.; Merayo, N.; Campano, C.; Negro, C.; Blanco, A. Industrial application of nanocelluloses in papermaking: A review of challenges, technical solutions, and market perspectives. *Molecules* **2020**, *25*, 526. [[CrossRef](#)] [[PubMed](#)]
37. Wang, W.; Gu, F.; Deng, Z.; Zhu, Y.; Zhu, J.; Guo, T.; Song, J.; Xiao, H. Multilayer surface construction for enhancing barrier properties of cellulose-based packaging. *Carbohydr. Polym.* **2021**, *255*, 117431. [[CrossRef](#)] [[PubMed](#)]
38. Spence, K.L.; Venditti, R.A.; Rojas, O.J.; Habibi, Y.; Pawlak, J.J. The effect of chemical composition on microfibrillar cellulose films from wood pulps: Water interactions and physical properties for packaging applications. *Cellulose* **2010**, *17*, 835–848. [[CrossRef](#)]
39. Chanda, S.; Bajwa, D.S. A review of current physical techniques for dispersion of cellulose nanomaterials in polymer matrices. *Rev. Adv. Mater. Sci.* **2021**, *60*, 325–341. [[CrossRef](#)]
40. Sundar, N.; Stanley, S.J.; Kumar, S.A.; Keerthana, P.; Kumar, G.A. Development of dual purpose, industrially important PLA-PEG based coated abrasives and packaging materials. *J. Appl. Polym. Sci.* **2021**, *138*, 50495. [[CrossRef](#)]
41. Pego, M.F.F.; Bianchi, M.L.; Yasumura, P.K. Nanocellulose reinforcement in paper produced from fiber blending. *Wood Sci. Technol.* **2020**, *54*, 1587–1603. [[CrossRef](#)]
42. Hii, C.; Gregersen, Ø.W.; Chinga-Carrasco, G.; Eriksen, Ø. The Effect of MFC on the Pressability and Paper Properties of TMP and GCC Based Sheets. *Nord. Pulp Pap. Res. J.* **2012**, *27*, 388–396. [[CrossRef](#)]

43. Butt, H.-J.; Liu, J.; Koynov, K.; Straub, B.; Hinduja, C.; Roismann, I.; Berger, R.; Li, X.; Vollmer, D.; Steffen, W.; et al. Contact angle hysteresis. *Curr. Opin. Colloid Interface Sci.* **2022**, *59*, 101574. [\[CrossRef\]](#)
44. Wang, X.Y.; Tian, W.; Ye, Y.H.; Chen, Y.; Wu, W.J.; Jiang, S.H.; Wang, Y.L.; Han, X.S. Surface modifications towards superhydrophobic wood-based composites: Construction strategies, functionalization, and perspectives. *Adv. Colloid Interface Sci.* **2024**, *326*, 103142. [\[CrossRef\]](#)
45. Barrino, F.; Ramírez, H.D.L.R.; Schiraldi, C.; Martínez, J.L.; Samper, M.D. Preparation and Characterization of New Bioplastics Based on Polybutylene Succinate (PBS). *Polymers* **2023**, *15*, 1212. [\[CrossRef\]](#)
46. Shi, K.; Ma, Q.; Su, T.; Wang, Z. Preparation of porous materials by selective enzymatic degradation: Effect of in vitro degradation and in vivo compatibility. *Sci. Rep.* **2020**, *10*, 7031. [\[CrossRef\]](#) [\[PubMed\]](#)
47. Dufresne, A. *Nanocellulose: From Nature to High Performance Tailored Materials*; Walter de Gruyter: Berlin, Germany, 2013.
48. Feng, L.; Li, S.; Li, H.; Zhai, J.; Song, Y.; Jiang, L.; Zhu, D. Super-Hydrophobic Surface of Aligned Polyacrylonitrile Nanofibers. *Angew. Chem. Int. Ed.* **2002**, *41*, 1221–1223. [\[CrossRef\]](#)
49. Zhang, X.; Liu, X.; Laakso, J.; Levänen, E.; Mäntylä, T. Easy-to-Clean Property and Durability of Superhydrophobic Flaky γ -Alumina Coating on Stainless Steel in Field Test at a Paper Machine. *App. Surf. Sci.* **2012**, *258*, 3102–3108. [\[CrossRef\]](#)
50. Fowkes, F.M. Attractive forces at interfaces. *Ind. Eng. Chem.* **1964**, *56*, 40–52. [\[CrossRef\]](#)
51. Adamson, A.W. *Physical Chemistry of Surfaces*, 5th ed.; Wiley & Sons: New York, NY, USA, 1976; p. 377.
52. Semple, K.E.; Zhou, C.; Rojas, O.J.; Nkeuwa, W.N.; Dai, C. Moulded Pulp Fibers for Disposable Food Packaging: A State-of-the-Art Review. *Food Packag. Shelf Life* **2022**, *33*, 100908. [\[CrossRef\]](#)
53. Liu, L.; Lei, Y.; Chen, G. Research on the Preparation and Properties of Water Resistant and Oil Resistant Paper Tableware Made by Bagasse Brown Pulp. In *Applied Sciences in Graphic Communication and Packaging*; Zhao, P., Ouyang, Y., Xu, M., Yang, L., Ren, Y., Eds.; Lecture Notes in Electrical Engineering; Springer: Singapore, 2018; Volume 477, pp. 609–615. ISBN 978-981-10-7628-2.
54. Bonfatti Júnior, E.A.; Raia, R.Z.; Bila, N.F.; Lopes, M.S.; Klock, U.; Andrade, A.S.; Vivian, M.A. Kraft pulping and papermaking of *Cryptomeria japonica*. *Sci. Fores.* **2019**, *47*, 811–822. [\[CrossRef\]](#)
55. Brodin, F.W.; Gregersen, Ø.W.; Syverud, K. Cellulose Nanofibrils: Challenges and Possibilities as a Paper Additive or Coating Material—A Review. *Nord. Pulp Pap. Res. J.* **2014**, *29*, 156–166. [\[CrossRef\]](#)
56. Mtibe, A.; Liganiso, L.Z.; Mathew, A.P.; Oksman, K.; John, M.J.; Anandjiwala, R.D. A comparative study on properties of micro and nanopapers produced from cellulose and cellulose nanofibres. *Carbohydr. Polym.* **2015**, *118*, 1–8. [\[CrossRef\]](#)
57. Wang, H.; Wang, J.; Si, S.; Wang, Q.; Li, X.; Wang, S. Residual-Lignin-Endowed Molded Pulp Lunchbox with a Sustained Wet Support Strength. *Ind. Crops Prod.* **2021**, *170*, 113756. [\[CrossRef\]](#)
58. Thanakkasaranee, S.; Sadeghi, K.; Seo, J. Packaging materials and technologies for microwave applications: A review. *Crit. Rev. Food Sci. Nutr.* **2022**, *63*, 6464–6483. [\[CrossRef\]](#) [\[PubMed\]](#)
59. Majder-Łopatka, M.; Węsierski, T.; Ankowski, A.; Ratajczak, K.; Durski, D.; Piechota-Polanczyk, A.; Polanczyk, A. Thermal Analysis of Plastics Used in the Food Industry. *Materials* **2022**, *15*, 248. [\[CrossRef\]](#) [\[PubMed\]](#)
60. Mofokeng, J.P.; Luyt, A.S.; Tábi, T.; Kovács, J. Comparison of injection moulded, natural fibre-reinforced composites with PP and PLA as matrices. *J. Thermoplast. Compos. Mater.* **2012**, *25*, 927–948. [\[CrossRef\]](#)
61. Hu, X.; Su, T.; Li, P.; Wang, Z. Blending modification of PBS/PLA and its enzymatic degradation. *Polym. Bull.* **2018**, *75*, 533–546. [\[CrossRef\]](#)

Disclaimer/Publisher's Note: The statements, opinions and data contained in all publications are solely those of the individual author(s) and contributor(s) and not of MDPI and/or the editor(s). MDPI and/or the editor(s) disclaim responsibility for any injury to people or property resulting from any ideas, methods, instructions or products referred to in the content.